Chemistry
A European
Journal

Chemistry
Europe
European Chemical
Societies Publishing

Title: Aryl Triflates in On-Surface Chemistry

Authors: Jindong Ren, Henning Klaasen, Melanie C. Witteler, Lena Viergutz, Johannes Neugebauer, Hong-Ying Gao, Armido Studer, and Harald Fuchs

To be cited as: *Chem. Eur. J.* 10.1002/chem.202002486

Link to VoR: https://doi.org/10.1002/chem.202002486

WILEY-VCH

Chemistry - A European Journal

10.1002/chem.202002486

WILEY-VCH

FULL PAPER

Aryl Triflates in On-Surface Chemistry

Jindong Ren,[a, b, #] Henning Klaasen,[c, #] Melanie C. Witteler,[c, d] Lena Viergutz,[c] Johannes Neugebauer,[c, d] Hong-Ying Gao,*[a, b, e] Armido Studer*[c] and Harald Fuchs*[a, b, f]

[a] Dr. J. Ren, Dr. H.-Y. Gao, Prof. Dr. H. Fuchs
Center for Nanotechnology (CeNTech)
Heisenbergstraße 11, 48149 Münster (Germany)
E-mail: gaoh@wwu.de, fuchsh@wwu.de
[b] Dr. J. Ren, Dr. H.-Y. Gao, Prof. Dr. H. Fuchs
Physikalisches Institut
Westfälische Wilhelms-Universität
Wilhelm-Klemm-Straße 10, 48149 Münster (Germany)
[c] Dr. H. Klaasen, M. C. Witteler, L. Viergutz, Prof. Dr. J. Neugebauer, Prof. Dr. A. Studer
Organisch-Chemisches Institut
Westfälische Wilhelms-Universität
Corrensstraße 40, 48149 Münster (Germany)
[d] M. C. Witteler, Prof. Dr. J. Neugebauer
Center for Multiscale Theory and Computation
Westfälische Wilhelms-Universität
Corrensstraße 40, 48149 Münster (Germany)
[e] Dr. H.-Y. Gao
School of Chemical Engineering and Technology
Tianjin University
Tianjin 300072 (China)
[f] Dr. H. Fuchs
Herbert Gleiter Institute of Nanoscience
Nanjing University of Science and Technology
Xiaolingwei 200, 210094 Nanjing (P. R. China)
[#] These authors contributed equally to this work.

Supporting information for this article is given via a link at the end of the document.

Abstract: The reactivity of aryl triflates in on-surface C-C coupling is reported. It is shown that the triflate group in aryl triflates enables regioselective homo coupling with preceding or concomitant hydro-detriflation on Cu(111). Three different symmetrical π-systems with two and three triflate functionalities were used as monomers leading to oligomeric conjugated π-systems. The cascade, comprising different intermediates at different reaction temperatures as observed for one of the molecules, proceeds via initial removal of the trifluoromethyl sulfonyl group to give an aryloxy radical which in turn is deoxygenated to the corresponding aryl radical. Thermodynamically driven regioselective 1,2-hydrogen atom transfer leads to a translocated aryl radical which in turn undergoes coupling. For a sterically more hindered bistriflate, where one *ortho* position was blocked, dehydrogenative coupling occurred at remote position with good regioselectivity. Starting materials, intermediates as well as products were analysed by scanning tunneling microscopy. Structures and suggested mechanism were further supported by DFT calculations.

Introduction

The identification of novel reactive functionalities is key for the further development of on-surface chemistry.[1] Considering the on-surface activation of σ-bonds, C–X bonds in aryl halides have found particular attention. Especially, the mechanism of the Ullmann coupling[2] comprising such an aryl–X activation is well understood. It was found that the energy barrier for splitting of bromine and iodine atoms from the corresponding halogenated precursors is reduced by interaction with the surface, with the largest impact found by the Cu(111) surface.[3] The resulting radicals are usually expected to be stabilized by bonding to the supporting surface[3,4] or to halogen adatoms[5] that are adsorbed between surface and this reactive intermediate. As the temperature raises, adatoms stabilize these radicals by formation of metal organic coordination complexes, as observed in experimental studies[6-8] and predicted by theoretical analysis.[7,8] Recently, it was even possible to visualize different intermediates of the Ullmann coupling by nc-AFM with a CO functionalized tip.[4,8] This strategy has also been used to better describe the mechanism of other on-surface processes such as decarboxylative coupling,[9] Glaser coupling,[10] Bergmann reaction[11] and carbene coupling.[12] In order to expand the scope of the Ullmann coupling, variations of the reactive starting unit have been disclosed. For example, coupling reactions of organic halides that vary in carbon hybridization state have been developed[13] and the reactivity of aryl chlorides was investigated.[14] However, aryl triflates, which show a similar reactivity as aryl halides in transition metal catalysed coupling processes in solution, have so far not been studied in on-surface chemistry. Due to their ready preparation, we regarded them as interesting starting materials also for on-surface chemistry.

Herein we present the on-surface self-assembly behaviour and reactivity of three different aryl triflates **TPTB 1** (1,3,5-tris (phenyl-4-trifluoromethylsulfonate)benzene), **BDBT 2** (biphenyl-4,4'-diyl bis(trifluoromethylsulfonate)) and **QDBT 3** (*m*-quaterphenyl-4’,6’’-diyl-bis(trifluoromethylsulfonate)) on the Cu(111) surface (Scheme 1a). It

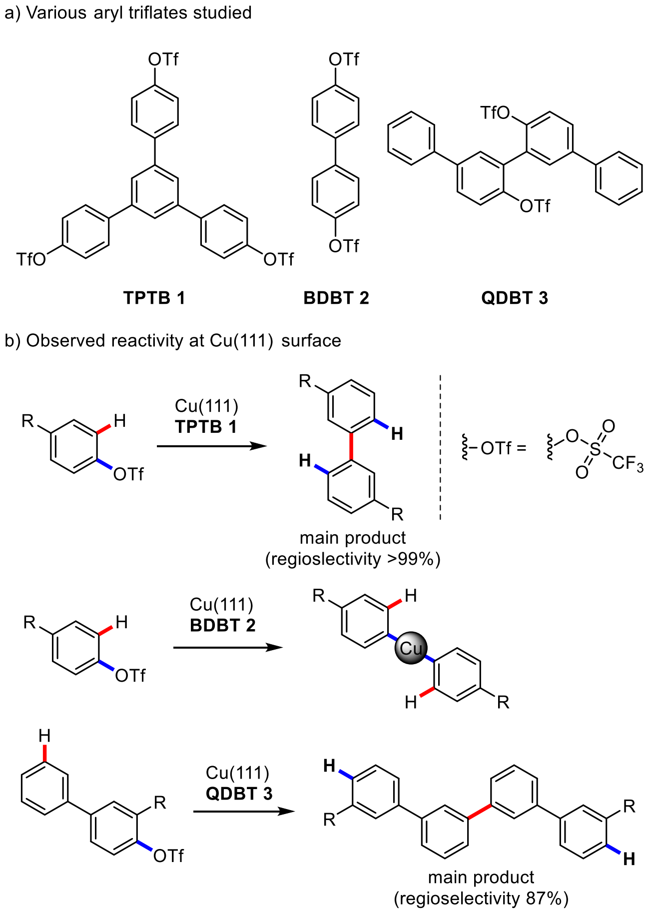

Scheme 1. Monomers used in the present study as well as observed reactivity.

is shown that the triflate moiety under ultra-high vacuum (UHV) conditions undergoes *ortho* homocoupling, as investigated by scanning tunnelling microscopy (STM) (Scheme 1b). Concomitant with the C-C coupling, removal of the triflate moiety (hydrodetriflation) is occurring. If the sterically more hindered *ortho* substituted **QDBT 3** is used, remote C–H functionalization at neighbouring phenyl substituents was observed as dominant reaction pathway. Upon annealing, linear polymer chains were formed resulting from a templating effect of the remaining triflate fragments that can be removed after the coupling reactions under comparably mild conditions, demonstrating the potential of bis and tris(triflates) as monomers in surface assisted polymerization.

Results and Discussion

We first tested **TPTB 1** (the syntheses of all triflates are described in the ESI) on the Cu(111) surface at different annealing temperatures (Fig. 1). After deposition at room temperature (300 K) with a base pressure of $4.5\text{x}10^{-10}$ mbar and cooling to 78 K for STM analysis, disordered self-assembled structures were formed (Fig. S1). Upon annealing at 370 K formation of a C_3-symmetric structure made of six molecules in its unit cell ($a = b = 2.45 \pm 0.06$ nm, $\theta = 60 \pm 0.5°$) and Y shaped pores was observed (Fig. 1a). Within the hexameric units two orientations of the molecules were found, where every second molecule is rotated by 30°. As this structure contains smaller adsorbates, an activation of the triflate functionality is proposed leading to aryloxy radicals **R1** (Fig. 1b and c) that have previously been generated from phenols on Au(111) and Ag(111) surfaces.[15] In lateral measurement a distance of 0.86 ± 0.05 nm between a central benzene ring and the connecting point to a neighbouring molecule was found (for method and corresponding line profiles of all distance measurements concerning **TPTB 1** see Fig. S2). This distance and the angle at the connecting points led to the assumption that the oxygen atom in aryloxy radicals **R1** bind to Cu adatoms which could stabilize the structure. This model was also investigated by DFT calculations and the expected distance of 0.83-0.86 nm between a central benzene ring and a Cu adatom fits the experimental data very well (Fig. S3).

Further annealing of the sample at 405 K led to a hexagonal honeycomb lattice (Fig. 1d). The high-resolution STM image revealed the molecular arrangement depicted in Fig. 1e. Between the molecules a circular protrusion connecting the adjacent molecular units could be distinguished and ascribed to Cu adatoms.[16] The angle of 180° at the connecting moieties supported the assumption that the C–O bond was cleaved leading to aryl radicals **R2** (Fig. 1f) connected by adatoms. Unlike reported aryloxy radical C–C couplings on Au(111) and Ag(111),[15] deoxygenation of the aryloxy radical on Cu(111) is faster than *ortho* homocoupling. The existence of Cu adatom stabilized radicals **R2** was further supported by distance measurement between two central benzene rings in the observed STM line profile, which was measured to be 1.49 ± 0.05 nm fitting the proposed structure well (Fig. S4). Notably, individual deoxygenated aryl radicals **R3** (Fig. 1i) most probably stabilized by tilting and binding to the surface were also observed within the pores of the honeycomb structure. These could either be radicals **R2** unattached to adatoms, or, similar to previously reported work, translocated *m*-arylphenylradicals originating from a 1,2-hydrogen atom transfer (HAT).[17]

Upon further annealing at 440 K for 20 min, individual aryl radicals of type **R3** were found to be the dominant species at the surface in a self-assembly ($a = b = 1.67 \pm 0.05$ nm, $\theta = 60 \pm 0.5°$) arranged in parallel pointing in the same direction with no adatoms being identified (Fig. 1g). The intermolecular distance between the phenyl rings located at the nodes was measured to be 0.98 ± 0.05 nm. In a theoretical model containing three molecules of **R3** type coordinating to a Cu atom, the distance between the same phenyl rings was found to be 0.58-0.59 nm. Further, in a model conceived on the basis of the experimental distances containing a Cu adatom, the C–Cu bond length would exceed the calculated bond length of 0.20-0.21 nm by more than 0.2 nm, further supporting the absence of adatoms in the structure formed at 440 K (for calculations and extended discussion see Fig. S5). In the high-resolution image, the observed distorted topography indicates the proposed 1,2-HAT (Fig. 1h).

To support our assumption of the translocation in triradical **R3**, the adsorption geometry was carefully investigated (Fig. S6). The four possible combinations of the radical centres being either in *para* or in *meta* position were calculated and the corresponding total energies and adsorption energies were compared. The calculations revealed that the most stable conformation is achieved when all radicals are localized at the *meta* position. All-*meta*-**R3** is 81 kJ/mol more stable in comparison to all-*para*-**R3** and also the adsorption on the Cu(111) surface is about 75 kJ/mol stronger. As the surface coverage remained unaltered during annealing and both phases coexist afterwards, it is highly likely

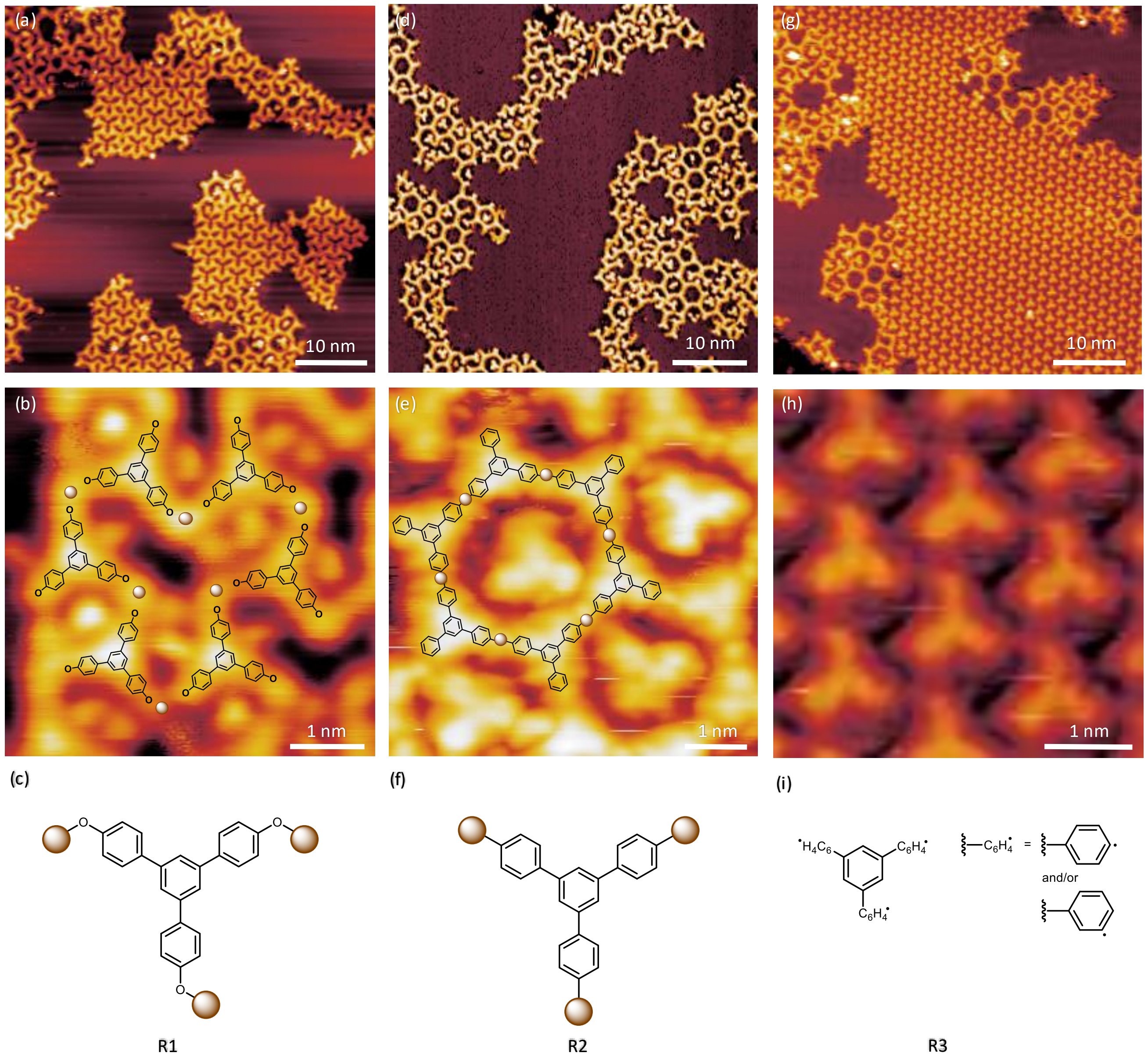

Figure 1. STM topographies of organometallic structures constructed by TPTB 1 on Cu(111) surface at different annealing temperatures. (a) Overview and (b) high-resolution STM image recorded after annealing at 370 K for 20 min. (c) Proposed structure observed in (a) and (b). (d) Overview and (e) high-resolution STM image recorded after annealing at 405 K for 20 min. (f) Proposed structure observed in (d) and (e). (g) Overview and (h) high-resolution STM image recorded after annealing at 440 K for 20 min. (i) Proposed structure observed in (g) and (h). Chemical sketches represent the respective dominantly formed radical species that are stabilized by bonding to the substrate or adatoms. All STM images were acquired with a tunneling current of I = –0.2 nA and a voltage of Vb = –2.0 V.

that the radicals **R3** were gradually generated from Cu adatom stabilized radicals **R2**.

At even higher temperature (470 K), oligomerization was observed (Fig. 2). As can be seen in the overview image, rearranged aryl radicals engaged in coupling reactions and disordered oligomers were formed (Fig. 2a). The high-resolution STM images show that the molecules are even closer together than in the organometallic network, suggesting covalent bond formation via radical/radical coupling (Figs. 2b and c). Distance measurement of the formed macrocycle (Fig. 2b) revealed a diameter of 0.84 nm ± 0.06 nm in good agreement with the structure optimized by DFT calculations (0.85 nm and 0.87 nm) (Fig. S7). Notably, the molecules were connected *ortho* to the former triflate groups with excellent regioselectivity showing that the 1,2-HAT is an efficient process at temperatures between 440 K and 470 K. Thus, a variation of the known *ortho* coupling of phenols that is so far restricted to Au(111) and Ag(111) surfaces has been performed at the Cu(111) surface.[15] For the reported phenol coupling on Au(111) and Ag(111) surfaces, C–C bond formation was suggested to occur prior to C–O cleavage as supported by calculations. This is unlike the current case on Cu(111) starting with triflates, where deoxygenation occurs prior to C–C coupling and regioselectivity is based on a thermodynamically favoured 1,2-H shift. It is currently not understood why the C–C coupling in these aryl radicals did not occur from the non-rearranged radicals derived from **R2**. Notably, using a *meta* derivative of **TPTB 1**, 1,3,5-tris (phenyl-3-trifluoromethylsulfonate)benzene, it was not possible to perform

10.1002/chem.202002486

the same reaction cascade. While the structures observed on surface do not change at temperatures between 370 K and 440 K, decomposition was observed at 470 K (Fig. S8). We also tested the reactivity of **TPTB 1** on Ag(111) where the formation of a highly ordered self-assembled structure of aryl radicals was already observed at room temperature (Fig. S9). At higher annealing temperatures, only the decomposition of the radicals generated at the surface was noted.

With biphenyl-4,4'-diyl bis(trifluoromethylsulfonate) **BDBT 2** as the starting material on Cu(111), long linear organometallic chains were formed at room temperature, resulting from removal of the trifluoromethyl sulfonyl groups and subsequent deoxygenation of the aryloxy radicals (Fig. S10). The remaining trifluoromethyl sulfonyl fragments were located between the chains, enabling via a template effect the high order and low degree of defects along the chains. The organometallic chains formed from **BDBT 2** on Cu(111) seem to be very stable, as the structure does not change upon annealing at 375 K. However, at 440 K the topography changes and unidentified structures were observed. Aryl radical coupling products or products derived from HAT with subsequent coupling could not be identified.

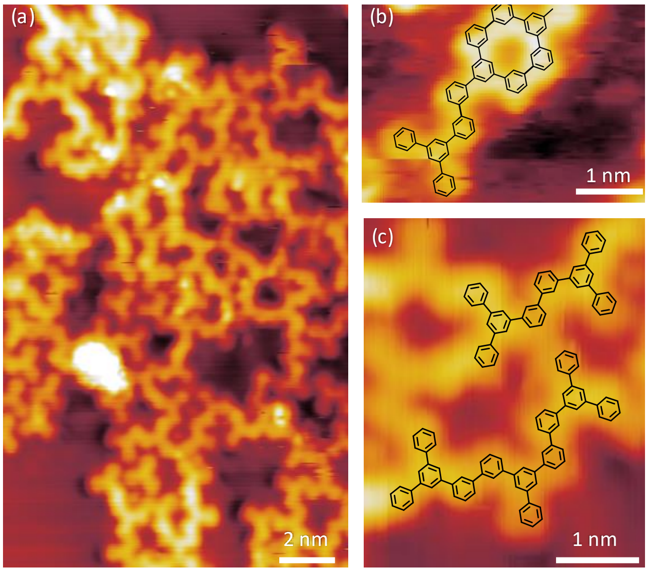

Figure 2. (a) STM overview image of covalent structures formed after annealing at 470 K for 20 min. (b-d) High-resolution images and corresponding molecular models of the proposed product structures. All STM images were acquired with a tunneling current of I = –0.48 nA and a voltage of Vb = –1.8 V.

We were further interested in the reactivity of an *ortho* substituted triflate to understand if *ortho* coupling is also possible on sterically more hindered precursors. To this end, ~0.7 ML **QDBT 3** was evaporated onto a Cu(111) surface kept at 300 K (Fig. 3). In the STM image, formation of two ordered phases, which consist of linear chains (phase I, Fig. 3b) and paired dimers (phase II, Fig. 3c), was observed. Due to rotation around the C–C bond linking the two biphenyl moieties, two distinct adsorption geometries, imaged as linear or kinked shape, are possible and self-sorting leads to the two phases. In phase I, molecules adsorbed with linear geometry self-assembled in chains composed of both enantiomers arranged alternatingly (Fig. 3b). Molecules adsorbed in kinked geometry prefer to form head-to-head dimers in phase II (Fig. 3c). Even though no triflate fragments were observed and stability of **QDBT 3** towards thermal evaporation was confirmed by in situ EI-MS experiments, the short distance between the two adsorbates found in phase II leads to the assumption that some or all triflate groups in this phase might be split off the backbone.

To study the on-surface reactivity of **QDBT 3**, we gradually annealed the sample and observed oligomeric structures along some individual adsorbates at 400 K (Fig. 3d). CF_3SO_2-groups were found to cleave from the monomers and are imaged as bright protrusions between the oligomeric chains (Fig. 3d). As only oligomerization products were identified, deoxygenation, HAT and coupling occurred sequentially at around the same temperature, unlike for the **TPTB 1** case discussed above. Therefore, aryloxy and aryl radicals could not be identified. In contrast to **TPTB 1**, C–C coupling occurred at remote position via the neighbouring phenyl groups, showing that multiple HAT had occurred prior to the aryl radical coupling steps. The sub-molecular resolution image presented in Fig. 3d clearly shows that the aryl/aryl linkages between the former monomers are located at the neighbouring phenyl ring, preferably at the *meta* positions leading to poly-*meta*-phenylenes.

Along the remote C–H functionalization events, few *ortho* coupling reactions were observed. As the monomeric precursor can adsorb in two different geometries, linear (L) and kinked (K), and coupling can occur in *ortho* (O) and in remote position (R), four possible reaction sites can be assigned (Fig. 3e top). A statistical analysis based on 560 C–C bond formations as obtained from STM images (30 x 30 nm²) revealed that the ratios of the L-O, L-R, K-O and K-R sites are 4%, 48%, 9% and 39%, respectively (Fig. 3e). It is currently assumed that stabilization of the radicals is favoured in remote position as bending of the molecule along the quaterphenyl backbone leads to a less distorted structure.

Notably, the lower reaction temperature in comparison to **TPTB 1** allows the sulfonyl fragments to remain at the surface. Their template effect enables the preparation of oligomers with a higher order.[18] Importantly, these sulfonyl fragments can post-synthetically be removed upon further increasing the temperature to 440 K (Fig. 3f). During this annealing step, even longer polymers were obtained and the CF_3SO_2-fragments probably decompose into gaseous by-products that leave the surface under UHV conditions. This is a highly interesting advance over the well-established Ullmann coupling, where bromine or iodine adatoms often disturb oligomerization[5] and can stay at the surface at annealing temperatures up to 540 K.[19]

We further performed lateral manipulation with the STM tip. It could be demonstrated that the topography of the polymer chain can be preserved after the tip operation (Fig. 3g and h). This indicates the strong coupling between the monomeric units and the phenyl-phenyl distance at the connection points further supporting the formation of covalent bonds. We also tested **QDBT 3** on Ag(111) surface. Unlike **TPTB 1**, only weak interaction between molecules and the substrate was observed and upon annealing most molecules leave the surface (Fig. S11).

Conclusion

In conclusion we have demonstrated both the self-assembly behaviour and on-surface reactivity of aryl triflates on Cu(111). In the case of a sterically less hindered monomer, the formation of self-assembled structures, organometallic networks and C–H functionalization was observed. Unlike previous works,[15] where phenols were found to form phenoxy radicals that undergo phenol

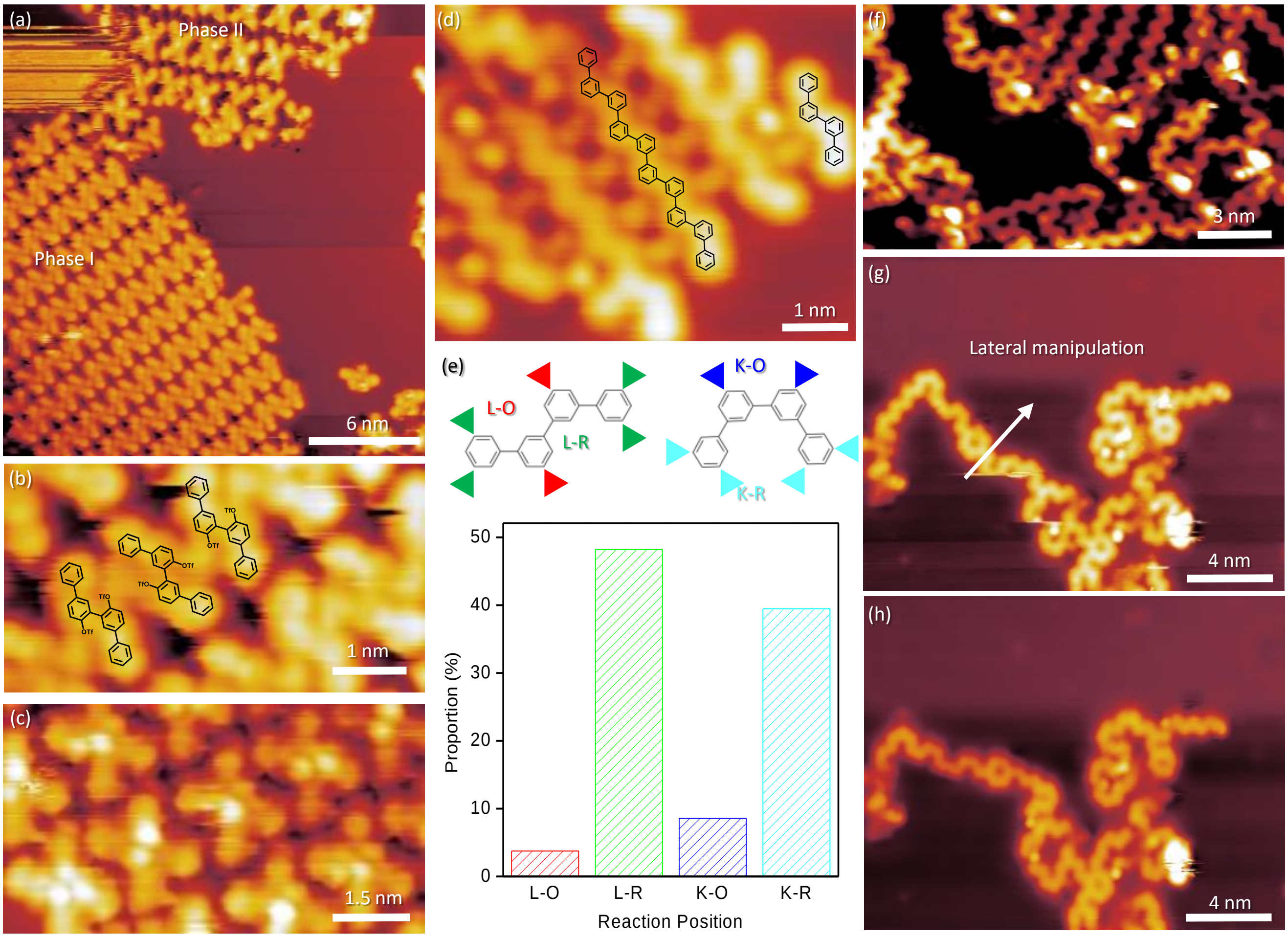

Figure 3. STM images of **QDBT 3** on a Cu(111) at different annealing temperatures, statistical analysis of reaction sites and lateral manipulation. (a) Overview image of the two coexisting phases I and II acquired with a tunneling current of I = –0.17 nA and a voltage of V_b = –2.1 V after deposition at RT. (b) and (c) High-resolution images of phase I and II, respectively. Both STM images are acquired with a tunneling current of I = –1.0 nA and a voltage of V_b = –2.1 V. (d) STM topography after annealing at 400 K acquired with a tunneling current of I = –1.0 nA and a voltage of V_b = –2.7 V. (e) Statistical analysis between ortho (O) and remote (R) C–H functionalization as well as linear (L) or kinked (K) geometry. (f) STM topography after annealing at 440 K acquired with a tunneling current of I = –0.3 nA and a voltage of V_b = –2.3 V. (g) and (h) Lateral manipulation of a polymer chain before and after operation. The white arrow in Fig. 3g represents the movement direction of STM tip during the manipulation. Image tunneling conditions: I = -0.60 nA; V_b = -4.6 V. Manipulation operation conditions: I = –8.0 nA; V_b = –0.03 V.

coupling in *ortho* position, the reaction series described above comprises cleavage of trifluoromethanesulfonyl groups, deoxygenation, 1,2-HAT and finally C–C coupling, as analysed by STM after annealing at different temperatures. When one *ortho* position is blocked as in **QDBT 3**, C–C coupling occurred preferably at a remote C–H position. Trifluoromethanesulfonyl fragments were found to facilitate templating effects to enable the preparation of polymers of higher order but can still be removed applying comparably mild conditions. We are confident that the triflate group will find further applications in on-surface chemistry in the future complementing the reactivity of phenols.

Acknowledgements

We thank the Deutsche Forschungsgemeinschaft (SFB 858, TRR 61) for financial support. H.-Y.G. thanks the NSFC within Grant 21972104 and “1000 Youth Talents Plan”.

Keywords: Aryl triflate • homo coupling • surface chemistry • STM • self-assembly

[1] a) P. A. Held, H. Fuchs, A. Studer, *Chem. Eur. J.* **2017**, *23*, 5874-5892; b) T. Wang, J. Zhu, *Sur. Sci. Rep.* **2019**, *74*, 97-140; c) S. Clair, D. G. de Oteyza, *Chem. Rev.* **2019**, *119*, 4717-4776; d) L. Grill, S. Hecht, *Nat. Chem.* **2020**, *12*, 115-130.

[2] a) L. Grill, M. Dyer, L. Lafferentz, M. Persson, M. V. Peters, S. Hecht, *Nat. Nanotechnol.* **2007**, *2*, 687-691; R. Gutzler, H. Walch, G. Eder, S. Kloft, W. M. Heckl, M. Lackinger, *Chem. Commun.* **2009**, 4456-4458; c) M. O. Blunt, J. C. Russell, N. R. Champness, P. H. Beton, *Chem. Commun.* **2010**, *46*, 7157-7159.

[3] J. Björk, F. Hanke, S. Stafström, *J. Am. Chem. Soc.* **2013**, *135*, 5768–5775.

[4] D. Ebeling, Q. Zhong, T. Schlöder, J. Tschakert, P. Henkel, S. Ahles, L. Chi, D. Mollenhauer, H. A. Wegner, A. Schirmeisen, *ACS Nano* **2019**, *13*, 324-336.

[5] A. Rastgoo Lahrood, J. Björk, W. M. Heckl, Markus Lackinger, *Chem. Commun.* **2015**, *51*, 13301-13304.

[6] M. Lischka, M. Fritton, J. Eichhorn, V. S. Vyas, T. Strunskus, B. V. Lotsch, J. Björk, W. M. Heckl, M. Lackinger, *J. Phys. Chem. C* **2018**, *122*, 5967-5977.

[7] D. Barton, H.-Y. Gao, P. A. Held, A. Studer, H. Fuchs, N. L. Doltsinis, J. Neugebauer, *Chem. Eur. J.* **2017**, *23*, 6190-6197.

[8] S. Zint, D. Ebeling, T. Schlöder, S. Ahles, D. Mollenhauer, H. A. Wegner, A. Schirmeisen, *ACS Nano* **2017**, *11*, 4183-4190.

[9] H.-Y. Gao, P. A. Held, M. Knor, C. Mück-Lichtenfeld, J. Neugebauer, A. Studer, H. Fuchs, *J. Am. Chem. Soc.* **2014**, *136*, 9658-9663.

[10] J. Liu, Q. Chen, Q. He, Y. Zhang, X. Fu, Y. Wang, D. Zhao, W. Chen, G. Q. Xu, K. Wu, *Phys. Chem. Chem. Phys.* **2018**, *20*, 11081-11088.

[11] A. Riss, A. P. Paz, S. Wickenburg, H.-Z. Tsai, D. G. De Oteyza, A. J. Bradley, M. M. Ugeda, P. Gorman, H. S. Jung, M. F. Crommie, A. Rubio, F. R. Fischer, *Nat. Chem.* **2016**, *8*, 678-683.

[12] L. Liu, H. Klaasen, A. Timmer, H.-Y. Gao, D. Barton, H. Mönig, J. Neugebauer, H. Fuchs, A. Studer *J. Am. Chem. Soc.* **2018**, *140*, 6000-6005.

[13] a) Q. Sun, L. Cai, Y. Ding, H. Ma, C. Yuan and W. Xu, *Phys. Chem. Chem. Phys.* **2016**, *18*, 2730-2735; b) Q. Sun, L. Cai, H. Ma, C. Yua, W. Xu, *Chem. Commun.* **2016**, *52*, 6009-6012; c) Q. Sun, L. Cai, H. Ma, C. Yuan, W. Xu, *ACS Nano* **2016**, *10*, 7023-7030; d) M. Liu, S. Li, J. Zhou, Z. Zha, J. Pan, X. Li, J. Zhang, Z. Liu, Y. Li, X. Qiu, *ACS Nano* **2018**, *12*, 12612-12618.

[14] a) K. J. Shi, X. Zhang, C. H. Shu, D. Y. Li, X. Y. Wu, P. N. Liu, *Chem. Commun.* **2016**, *52*, 8726-8729; b) K. J. Shi, D. W. Yuan, C. X. Wang, C. H. Shu, D. Y. Li, Z. L. Shi, X. Y. Wu, P. N. Liu, *Org. Lett.* **2016**, *18*, 1282-1285.

[15] a) Q. Li, B. Yang, H. Lin, N. Aghdassi, K. Miao, J. Zhang, H. Zhang, Y. Li, S. Duhm, J. Fan, L. Chi, *J. Am. Chem. Soc.* **2016**, *138*, 2809-2814; b) B. Yang, N. Cao, H. Ju, H. Lin, Y. Li, H. Ding, J. Ding, J. Zhang, C. Peng, H. Zhang, J. Zhu, Q. Li, L. Chi, *J. Am. Chem. Soc.* **2019**, *141*, 168-174.

[16] J. Ren, E. Larkin, C. Delaney, Y. Song, X. Jin, S. Amirjalayer, A. Bakker, S. Du, H. Gao, Y.-Y. Zhang, S. M. Draper, H. Fuchs, *Chem. Commun.* **2018**, *54*, 9305-9308.

[17] Q. Fan, S. Werner, J. Tschakert, D. Ebeling, A. Schirmeisen, G. Hilt, W. Hieringer, J. M. Gottfried, *J. Am. Chem. Soc.* **2018**, *140*, 7526-7532.

[18] J. Ren, M. Cnudde, D. Brunink, S. Buss, C. G. Daniliuc, L. Liu, H. Fuchs, C. A. Strassert, H.-Y. Gao, N. L. Doltsinis, *Angew. Chem.* **2019** *131*, 15542-15546; *Angew. Chem. Int. Ed.* **2019**, *58*, 15396-15400.

[19] C. Bronner, J. Björk, P. Tegeder, *J. Phys. Chem. C* **2015**, *119*, 486-493.

Entry for the Table of Contents

Insert graphic for Table of Contents here.

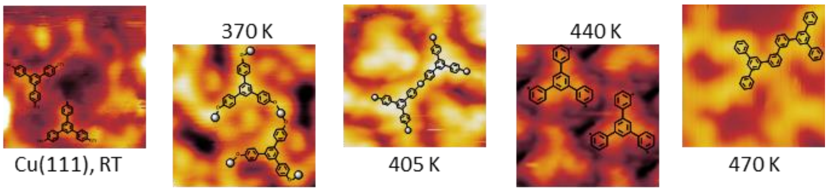

Insert text for Table of Contents here. **Step aside!** Coupling of aryl triflates, so far unknown in on-surface chemistry, is reported. Unlike aryl halides known in Ullmann coupling, aryl radicals formed from triflated monomers undergo HAT prior to C–C coupling, leading to unexpected regioselectivity. But not only H-atoms step aside: triflate fragments show a powerful templating effect during the reaction and leave the surface post-synthetically under mild conditions.